



## Climatology and Chemistry of Surface Ozone and Aerosol under Alpine Conditions in East Siberia

Vladimir L. Potemkin<sup>\*</sup>, Lydmila P. Golobokova, Tamara V. Khodzher

*Limnological Institute SB RAS, Irkutsk 664033, Russia*

---

### ABSTRACT

We present the results of synchronous observations of the ozone and gaseous impurity concentrations, chemical composition of the aerosol and meteorological parameters with a high temporal resolution (of minutes) at the background site Mondy, which is located in the highland area of East Siberia. We also analyzed the seasonal dynamics exhibited by the ozone, gaseous impurities of sulfur and nitrogen, and ionic composition of the aerosol over the long term (1998–2016). Ozone variability in the boundary layer depended on complicated relief and dynamic processes occurring in the atmosphere. The concentration of ions in the aerosol decreased by 2 times for the period of 2010–2015 compared to the beginning of the new millennium. Furthermore, sulfate, nitrate, chloride, potassium and sodium became the dominant ions in the aerosol. Due to the remote location of the site, the absence of anthropogenic pollution sources and the large series of data with different parameters obtained via on-line monitoring, this site may be regarded as a representative global background site for the vast region of Central Asia.

**Keywords:** East Sayan; Climatic parameters; Ozone; Aerosol; Troposphere.

---

### INTRODUCTION

Greenhouse gases and atmospheric aerosol are one of the most important factors of climate changes on the earth. Therefore, any additional experimental data on inter-annual variability of concentrations of these gases in different regions of the world will be of great interest. Long series of observations of gases in the surface atmosphere in a number of remote areas of the world available at present are still scarce. In this context, Siberia has remained as a “white spot” so far. Therefore, it was necessary to set up an atmospheric monitoring site under alpine conditions aimed at analyzing diurnal, seasonal and inter-annual dynamics of gaseous and aerosol components (Bashurova *et al.*, 1992; Pochanart *et al.*, 2003). One of the most suitable areas for such monitoring in the south of Siberia under background conditions of the continental climate was the Astronomic Observatory of the Institute of Solar-Terrestrial Physics of SB RAS, which is located near the settlement of Mondy (East Sayan, a mountain system of South Siberia; 51.6°N, 100.6°E; 2,005 m a.s.l.) (Pochanart *et al.*, 2003) (Fig. 1). This area is practically not subject to anthropogenic impact of local and regional sources and may represent inter-annual variability of regional and global background of greenhouse

gases. Since 2001, Limnological Institute of Siberian Branch of the Russian Academy of Sciences (Irkutsk, Russia) has been monitoring aerosol, atmospheric precipitation and some gases (O<sub>3</sub>, NH<sub>3</sub>, NO<sub>x</sub> and SO<sub>2</sub>) within the framework of the international program Acid Deposition Monitoring Network in East Asia (EANET) on the territory of this observatory. These observations allow us to compare the data obtained with the results from other regions of the world and to reveal specific characteristics of their variability under the background conditions of atmosphere on the vast territory of Siberia.

The studies of minor atmospheric gases provide important information for modeling and prediction of the future state of the earth's climatic system. Ozone is of great interest because of its high toxicity and chemical activity (Karlsson *et al.*, 2007). High spatial and time variability is characteristic of ozone concentration near the earth's surface. The rise and destruction of ozone are caused by local pollutants under urban conditions, whereas for the background areas natural reasons are more important.

We have selected meteorological parameters and daily values of ozone concentrations from January 1998 to January 2016 (a series length of 19 years) at the alpine site Mondy. Statistical functions of smoothing and linear correlations have been used for the investigations of the structure of an ozone series. We have also analyzed observations of other gaseous impurities and aerosol in the surface atmosphere in the background areas.

---

<sup>\*</sup> Corresponding author.

E-mail address: klimat@lin.irk.ru

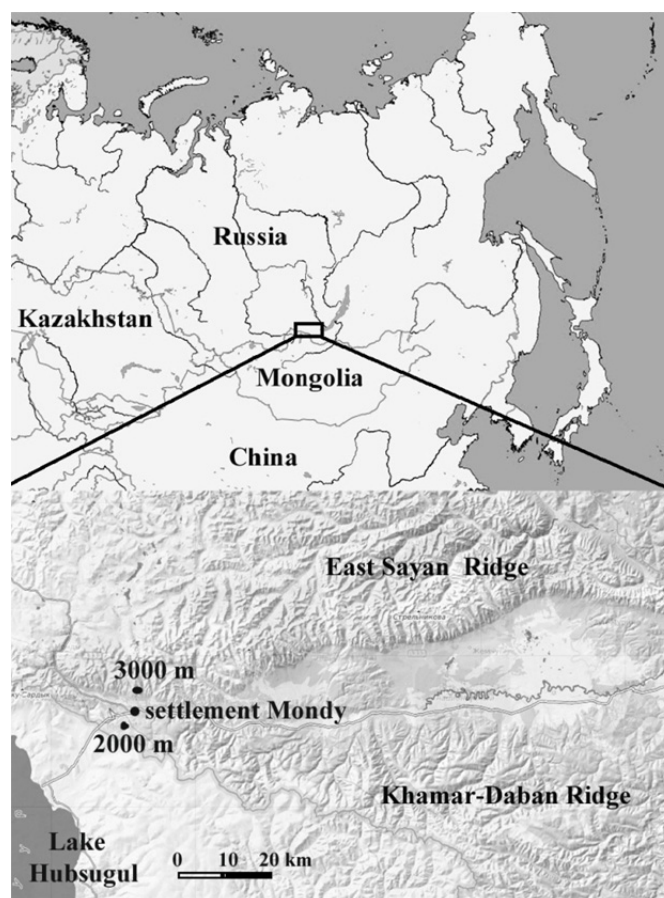


Fig. 1. The map of monitoring site.

## METHODS AND MATERIALS

The monitoring site is located at a distance of 200–300 km from the main industrial sources of atmospheric pollution, being surrounded by the system of the Large Sajan (3,491 m a.s.l., Mount Munku-Sadyk) from the west and southwest and by the ridges of the East Sajan (3,200–3,250 m a.s.l.) from the north and northwest. In the northeast and east, the site is surrounded by the Khamar-Daban Ridge (2,000–2,300 m a.s.l.). The southeastern and southern parts of the territory are surrounded by gentle hills of the same mountain system with the heights lower than 2,000 m. Atmospheric impurities enter site Mondy mainly as a result of natural soil-erosion processes, vegetation and forest fires. Dust storms from the arid zone of Mongolia, whose frequency has increased for the recent years, are the powerful source of alkaline components in aerosol (Lee and Sohn, 2011). The site is supplied with industrial electricity. There are no sources of atmospheric pollution at this site. Therefore, it is a representative place for observations of different meteorological parameters in the atmosphere under the background conditions. The nearest settlement Mondy (1,350 m a.s.l.) is located in the valley at a distance of several kilometers from the site. The data on meteorological observations presented in this work were obtained at the monitoring site and weather station in the settlement Mondy, as well as random data were

obtained at the additional observation point located in the East Sajan at 3,000 m a.s.l (Fig. 1).

Ozone concentrations in the surface atmosphere layer were measured on an ozone instrument, Dylec Model 1006-AHJ, with 10-minute averaging. The measurements were registered automatically on the computer with a device error of 10%. The instrument was calibrated once a year. Atmospheric pressure and air temperature were also registered synchronously in the room where the devices were installed (Pochanart *et al.*, 2003).

Aerosol and other gaseous impurities were sampled according to the methods applied in the international monitoring network EANET (Acid Deposition Monitoring Network in East Asia) and EMEP (European Monitoring and Evaluation Program). According to the *Technical Document for Filter Pack Method in East Asia* (Technical Manual, 2003), 4 types of filters were used for sampling. A filter holder with filters was hermetically connected to a pump and a gas meter.

Filters are set in the following order: PTFE, nylon, base-impregnated and acid-impregnated filters. The first Teflon PTFE filter (Filter 1) with 0.8  $\mu\text{m}$  in diameter was installed on the way of air flow for aerosol trapping. We identified  $\text{Ca}^{2+}$ ,  $\text{Mg}^{2+}$ ,  $\text{Na}^{+}$ ,  $\text{K}^{+}$ ,  $\text{NH}_4^{+}$ ,  $\text{NO}_3^{-}$ ,  $\text{Cl}^{-}$  and  $\text{SO}_4^{2-}$  in aqueous extracts of the first filter.  $\text{SO}_2$ ,  $\text{HNO}_3$ , and  $\text{NH}_3$  gases are collected by nylon (Filter 2), base-impregnated (Filter 3), and acid-impregnated filters (Filter 4), respectively.

In the aqueous extract of Filter 2, the ions  $\text{SO}_4^{2-}$ ,  $\text{NO}_3^-$ ,  $\text{Cl}^-$ ,  $\text{NH}_4^+$  were determined. Filter 3 was extracted with 0.05% hydrogen peroxide solution and the ions  $\text{SO}_4^{2-}$ ,  $\text{Cl}^-$  were determined. In the aqueous extract of Filter 4,  $\text{NH}_4^+$  ions were determined. The corresponding gaseous impurities of  $\text{SO}_2$ ,  $\text{HNO}_3$ , and  $\text{NH}_3$  were calculated and summarized from the concentrations of ions in the filtrates of Filters 2–4.

The sampling period took two weeks. There were 234 samples taken from 2000 to 2017.

To compare our data with the data from other regions of the world, we analyzed ions using sophisticated analytical methods recommended by the monitoring network: atomic absorption and high performance liquid and ionic chromatography (Ren *et al.*, 2012; Habeebullah *et al.*, 2016). Measurements were carried out on an atomic absorption spectrometer (Carl Zeiss Jena, Germany), high-performance liquid chromatographer (Milichrom A-02; Econova, Russia) and ionic system (ICS-3000; Dionex, USA). The quality of the analyses was verified by the participation in the inter-laboratory testing within the international programs of Global Atmospheric Watch (GAW) under the aegis of World Meteorological Organization (WMO) (Quality Assurance Science Activity Centres) and Acid Deposition Monitoring Network in East Asia (EANET). The laboratories performing chemical analysis are involved in the ACAP Network Centre's inter-laboratory comparison projects (on wet deposition, dry deposition and soil and inland aquatic environment monitoring (EANET, 1998–2015). The discrepancy between the results obtained and control values did not exceed 5–10%, which attested to the data validity (from the National Report).

### Climate of the Region

Alpine regions possess a specific type of climate called mountain climate; the height of the location significantly affects the distribution of meteorological parameters (Table 1). Mountain areas influence wind field in the boundary layer of troposphere perturbing the flux and promoting the development of the local circulation. At the monitoring site, due to more intense turbulence, mean wind speed is higher than in the valley; the largest difference ( $2\text{--}3\text{ m s}^{-1}$ ) is observed in the cold period at weakened mountain-valley circulation. The highest variations are recorded during intensification and destruction of the Asian maximum of atmospheric pressure with the sharp recurrent increase of the southern wind. The recurrence of the northern wind increases during transitional seasons at the transformation of the pressure field (Fig. 2).

Radiation and temperature regimes at this site have remained unchanged for two decades (Figs. 3–4). Air temperature was measured at three points of observations at 2,000 and 3,000 m and at the weather station at the settlement Mondy at 1,350 m a.s.l. (Fig. 4).

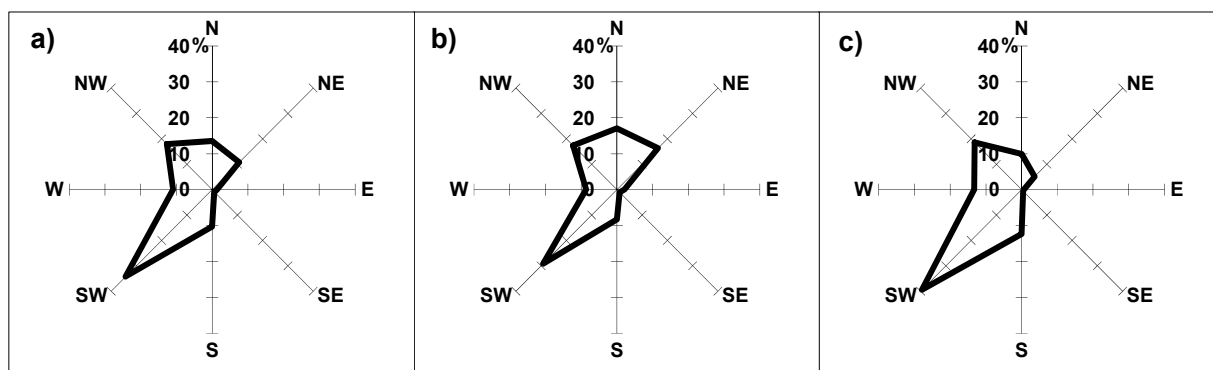
## STUDY AREA AND RESULTS

### Diurnal Variations of Ozone Concentration

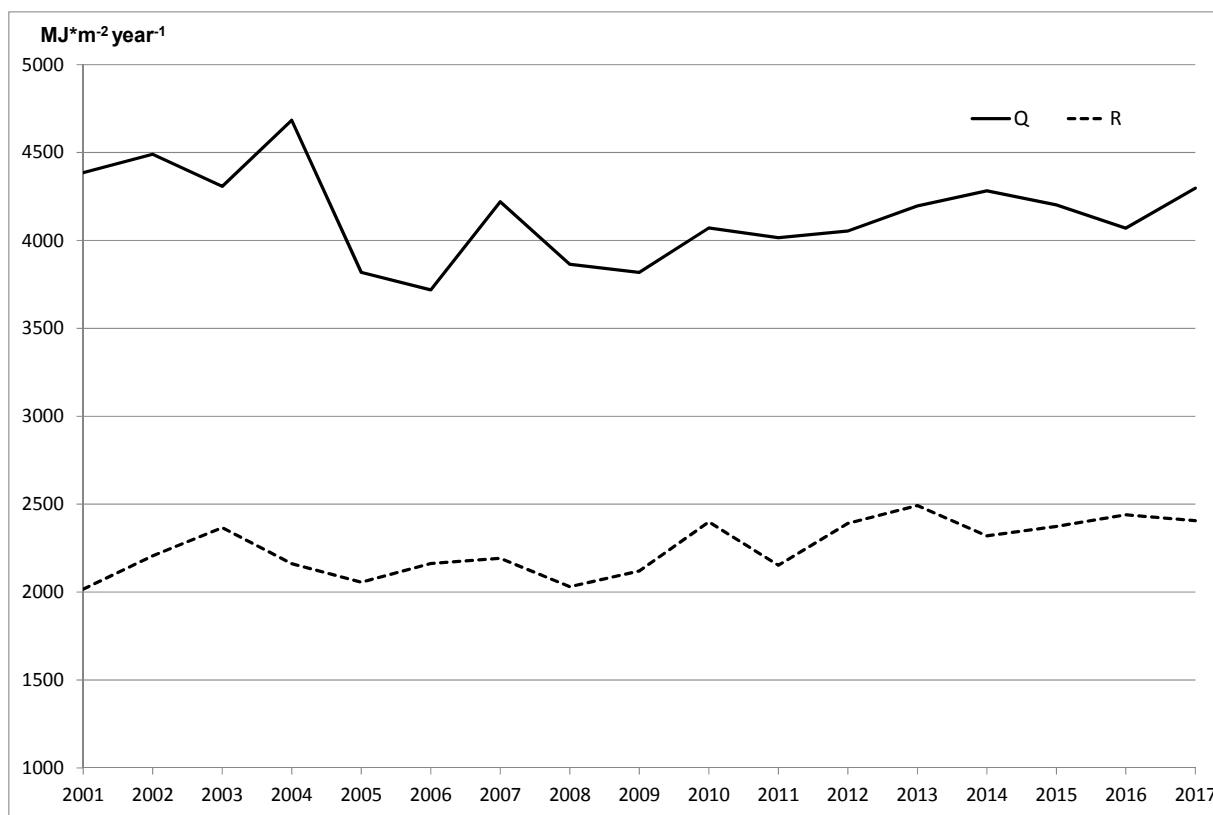
Average diurnal dynamics of the surface ozone concentration (SOC) were constructed for each season. In

Table 1. Average monthly meteorological data at site Mondy, 1998–2016.

Month													
Meteoroparameter	I	II	III	IV	V	VI	VII	VIII	IX	X	XI	XII	
Average temperature, (°C)	month	−22.0	−17.9	−10.0	0.4	6.8	13.3	14.7	12.3	7.3	−2.7	−13.4	−23.5
	max	−12.7	−8.0	0.6	8.5	16.1	21.2	22.1	20.9	17.9	5.9	−4.8	−15.4
	min	−28.7	−25.7	−19.6	−6.5	−1.9	5.5	8.9	5.7	−1.9	−10.0	−20.2	−29.4
Average humidity, (%)	month	73	68	58	53	62	65	73	80	75	61	69	68
	max	86	80	81	76	91	89	93	95	96	85	81	79
	min	48	49	37	35	40	43	48	58	48	36	48	50
Average wind speed (m s <sup>−1</sup> )	1.7	2.6	2.2	3.7	3.0	2.0	1.5	1.7	1.5	1.7	1.5	1.3	
Precipitation (mm month <sup>−1</sup> )	4.2	2.9	1.7	9.9	33.4	46.6	105.0	111.4	20.9	25.1	1.5	0.5	
Duration of solar light (hours)	168	212	270	243	296	265	276	199	214	180	143	150	
Solar radiation (MJ m <sup>−2</sup> month <sup>−1</sup> )	129	211	366	463	505	451	543	384	307	238	122	100	



**Fig. 2.** Wind-rose (frequency of wind directions, %) at site Mondy during a (a) year, (b) summer, and (c) winter.



**Fig. 3.** Inter-annual variability of total (Q) and direct (R) radiation.

all cases, minimal concentrations were recorded at night and morning hours and maximal at daytime and at evening hours. Diurnal SOC variability depended on dynamics of mixing layer and temperature inversions occurring at night.

At daytime, SOC variability was higher than at morning hours (Table 2, Fig. 5). This is attributed not only to photochemical generation of ozone in the surface atmosphere layer at daytime (Reddy *et al.*, 2012) but also to more intense air warming and turbulent exchange of air masses with the overlying atmosphere layers (Rovinsky and Egorov, 1986; Akimoto, 2006).

*January.* The diurnal trend was expressed insignificantly in January. The snow cover smoothed the diurnal trend of ozone concentration in the surface atmosphere layer as the destruction was less intense on its surface than on the

surface of the open ground. Minimal ozone concentrations were registered at 9–11 and maximal at 19, its diurnal variability being minimal with the 0.9 ppb amplitude. There was no photochemical generation of ozone.

*April.* Minimal concentrations of SOC were recorded in April at 10 and maximum at 17 with diurnal amplitude of 2.2 ppb. The increase of ozone concentrations was attributed to the total spring SOC maximum, which was recorded in April–May.

*July.* The highest amplitude and diurnal variability of SOC were recorded in July with its minimum at 8 and maximum from 13 to 16 with the 5.1 ppb amplitude. During this period, we observed a shift of SOC maximum relatively the noon maximum of the solar radiation due to the convective exchange of air masses in the second half of

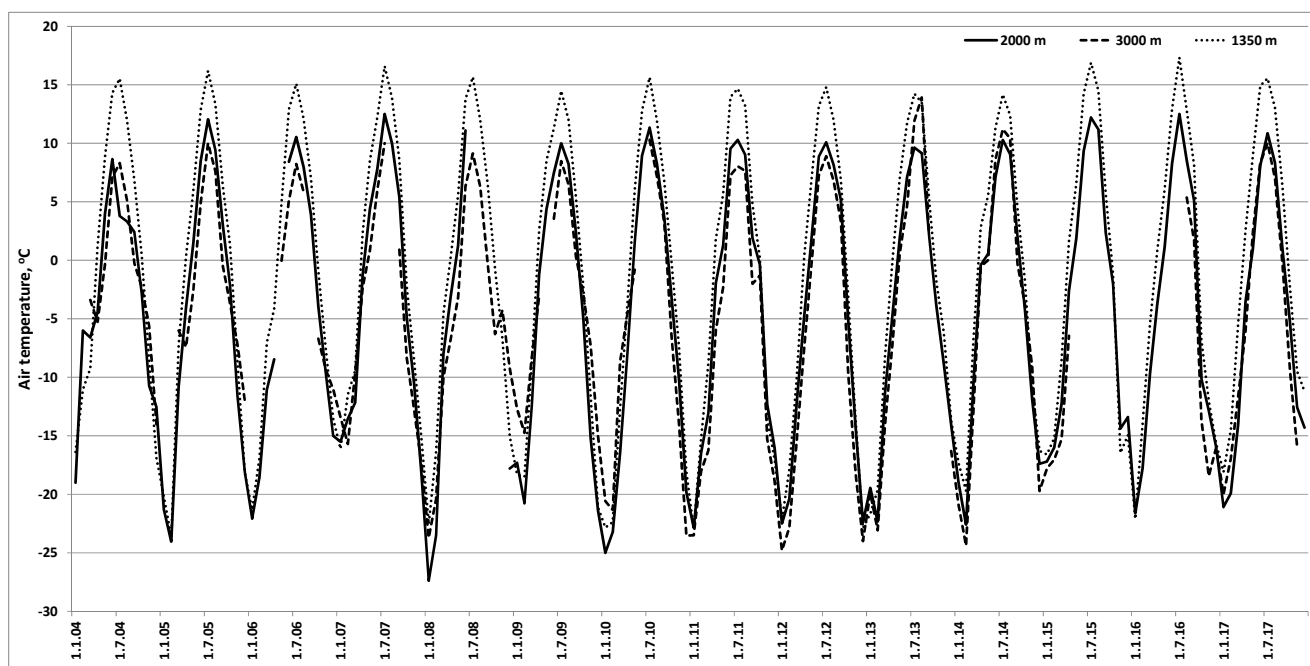


**Fig. 4.** Long-term dynamics of air temperature according to sites 2000 m, 3000 m and at weather station in the settlement Mondy (1350 m).

**Table 2.** Average long-term diurnal SOC dynamics in a season, 1998–2016.

season	Time of minimum, hours	Time of maximum, hours	Minimum, ppb	Maximum, ppb
January	9–11	19	$38.3 \pm 3.4$	$39.2 \pm 3.6$
April	10	17	$53.4 \pm 5.4$	$55.6 \pm 5.9$
July	8	13–16	$37.3 \pm 6.2$	$42.9 \pm 7.1$
October	9	16	$38.2 \pm 5.2$	$40.4 \pm 5.5$

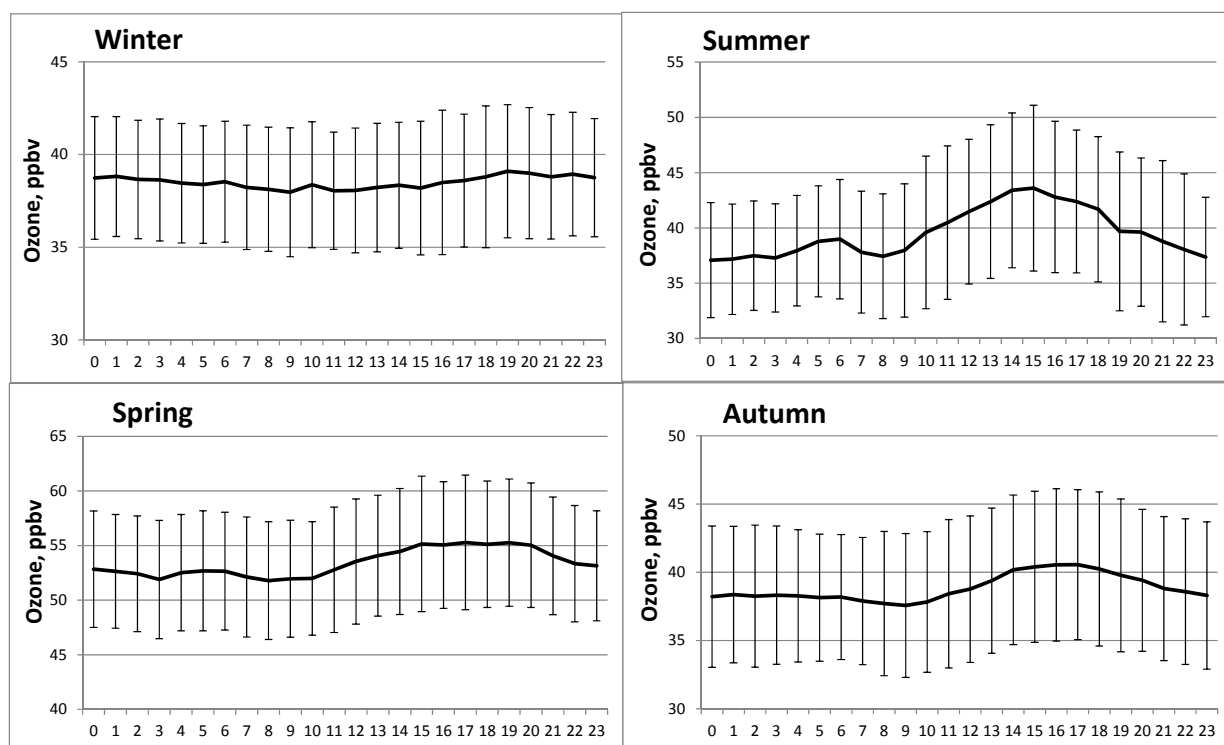


**Fig. 5.** Average diurnal SOC dynamics in a season.

the day and additional input of air enriched with ozone from the overlying layers to the earth surface. Although the main reason is the change in the duration of daylight hours and the constant presence of mountain circulation of air masses.

**October.** SOC minimum was registered in October at 9 and its maximum at 16 with the 2 ppb amplitude.

In the seasonal aspect, low and high diurnal variability of ozone concentrations was observed in the cold and warm seasons, respectively, which was attributed to the differences in destruction rate above different surfaces ( $0.02\text{--}0.03\text{ cm s}^{-1}$  on the snow cover and  $0.1\text{--}1.0\text{ cm s}^{-1}$  on the soil surface (Aldaz, 1969; Wesely *et al.*, 1981; Turner *et al.*, 1980; Laurila, 1999) and to the temperature difference. Moreover, this variability was caused by the interaction between ozone and biota (Karlsson *et al.*, 2007) and a great number of thunder days (Ozville, 1967). Diurnal amplitude of ozone varied from 0.5 to 1.0 ppb in a cold season (January) and from 5 to 8 ppb in a warm season (July).

### Seasonal Variation of Ozone Concentration

To study inter-annual dynamics of the ozone concentrations, we used a series of observations performed from January 1, 1998 (Fig. 6).

The seasonal variation of SOC had only one vividly expressed maximum recorded in late April–early May (the maximum varied from April 20 to May 19; Fig. 7).

There was no clearly defined minimum in the annual SOC trend. After the spring maximum, concentrations dropped up to the midsummer. Then, SOC values remained average without any clear maxima or minima up to the end of the year. The summer period was characterized by very high diurnal variability.

We should note that annual variability of SOC in the East Sayan corresponded to the dynamics characteristic of the whole Northern Hemisphere (Sandroni *et al.*, 1994; Laurila, 1999; Monks, 2000; Zanis *et al.*, 2007; Gilge *et al.*, 2010; Chen *et al.*, 2013).

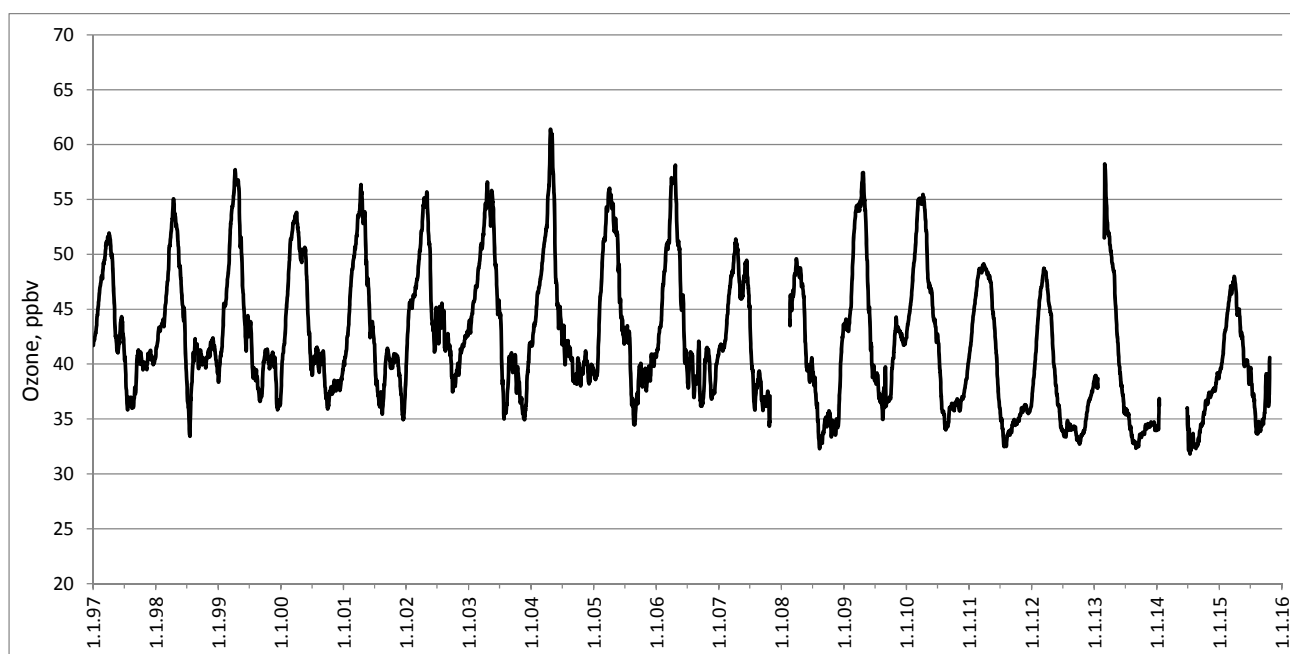


**Fig. 6.** Long-term changes in daily average ozone concentration near surface.

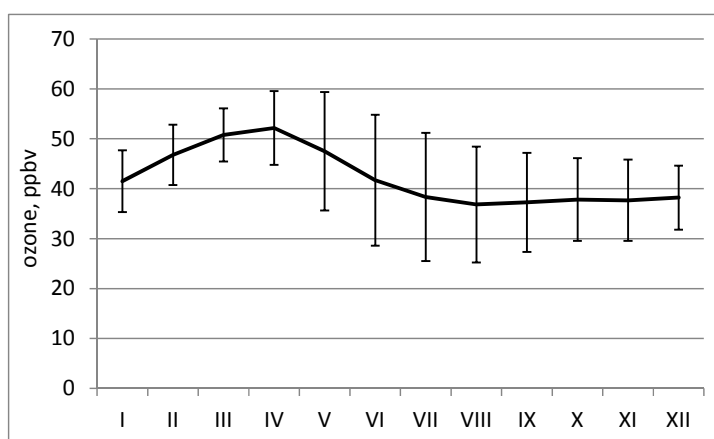


**Fig. 7.** Average seasonal variation of ozone concentration. The error bar is the standard deviation for each month.

Seasonal SOC variability was determined from the annual solar cycle as main sources of ozone formation were its sink from the upper troposphere (“ozone layer”) and photochemical reactions in the surface atmosphere layer. Processes occurring with the involvement of hydroxide radicals, nitrogen oxides and compounds of chloride and bromine contributed significantly to the ozone destruction (Belan, 2010). Spectral analysis confirmed the presence of two stable ozone cycles—annual and semi-annual (Fig. 8).

For this analysis, we averaged the series of diurnal ozone concentration with a 30-day period. Therefore, short-term synoptic cycles (4–7 days) were eliminated. It is obvious that an annual cycle depends on solar radiation, whereas a half-year cycle is determined from photochemical generation that depends on impurities (vegetation hydrocarbons) in the lower atmospheric layer and on meteorological parameters (elevated UV-radiation, temperature and humidity of air). This is characteristic of the monitoring site that is located on the upper border of the forest.

#### **Other Specific Characteristics of SOC Variability**

Abrupt changes in the SOC values are associated with the location of the monitoring site in the mountains with their unstable meteorological situation. Fig. 9 is an example of abrupt SOC changes happened on July 9, 2007, as a result of the wind direction change.

The monitoring site is located on the ridge, which separates the Tunkin Depression in the north from the basin of Lake Khubsugul in the south. The Tunkin Depression is 200 km long and about 10 km wide. The Lake Khubsugul basin is an even wide depression with large steppe slopes. The altitude difference between the site and the lake is 600–800 m. There are several settlements in the Tunkin Depression—Mondy (6 km from the site downwards the slope) and a larger settlement Kyren (60 km to the east from the site). The depression of Lake Khubsugul is almost uninhabited except temporary nomad camps. The SW stable wind of  $2\text{--}4\text{ m s}^{-1}$  was registered at noon hours. It brought

pure air enriched with ozone from the lake depression. At noon, the atmospheric pressure began dropping, and at 15:30 during several minutes the wind changed its direction—first northern, then northeastern (i.e., air masses from the Tunkin Depression and settlement Mondy entered the site area with significant ozone depletion). The wind speed was  $2\text{--}3\text{ m s}^{-1}$ . The ozone concentration dropped by 10–15 ppb. Such cases of abrupt changes in meteorological parameters were recorded at the site several times.

This example shows that abrupt changes in rise or drop of ozone concentration are possible with the duration of several hours. This is a very interesting phenomenon for the alpine region where mountain-valley circulations occur constantly because of the relief, which cause the exchange of huge air masses of different chemical composition.

#### **Dynamics of Aerosol Composition and Gaseous Impurities of Nitrogen and Sulfur**

We analyzed data of average long-term ionic composition of aerosol obtained within on-line monitoring in 2000–2017.

Table 3 lists long-term monthly average concentrations of ions in the aqueous extract of aerosol. The main ions are  $\text{SO}_4^{2-}$ ,  $\text{NH}_4^+$ ,  $\text{Ca}^{2+}$ ,  $\text{Na}^+$ ,  $\text{Cl}^-$ . Maximal concentrations of  $\text{SO}_4^{2-}$  and  $\text{NH}_4^+$  prevail during the cold period, maximal concentrations  $\text{Ca}^{2+}$ ,  $\text{Na}^+$ ,  $\text{Cl}^-$  prevail during the warm period. In long-term aspect, a change of chemical constitution of aerosol is being observed.

From 2000 to 2009, aerosol composition was dominated by  $\text{NH}_4^+$ ,  $\text{Ca}^{2+}$  and  $\text{SO}_4^{2-}$ , whereas in the following years, ionic composition of aerosol changed. In 2010–2015, the contribution of  $\text{Na}^+$ ,  $\text{K}^+$  and  $\text{Cl}^-$  significantly increased, whereas that of  $\text{NH}_4^+$  and  $\text{SO}_4^{2-}$  decreased. In 2015–2017, we again recorded the rise of  $\text{SO}_4^{2-}$ , the reason of which has not been elucidated so far.

The range of  $\text{NH}_4^+$  concentration was quantitatively higher (2–5 times) in 2000–2009 than in 2010–2015 (Fig. 10, Table 4). However, average long-term concentrations decreased by 5.9 times. The lower and upper limits of  $\text{SO}_4^{2-}$  concentrations decreased by 3.5 and 3.1 times, respectively, and average concentrations by 2.7 times. Smaller changes were recorded for  $\text{Ca}^{2+}$ : Lower and upper levels of concentrations decreased by 2.2 and 2.4 times, average value increased by 1.7 times (see Table 3).

The most significant changes in the concentration dynamics of ions were recorded for  $\text{Cl}^-$ . Average long-term lower and upper concentration limits of this ion increased by 23 and 2.6 times, respectively, and average long-term concentrations by 3.8 times. These changes for  $\text{Na}^+$  were 1.3, 3.5 and 2.5 times, respectively. Concentration ranges for  $\text{K}^+$  (2000–2009) practically did not change in 2010–2015, and average long-term concentrations increased insignificantly—by 1.2 times. However, the contribution of these ions increased from 2–5% to 5–12%.

Taking into consideration that radiation and temperature regimes in the region of observations have not practically changed during two decades, the main reasons affecting the changes of ionic composition of aerosol are intensifying climate aridization and increased number of dust storms in

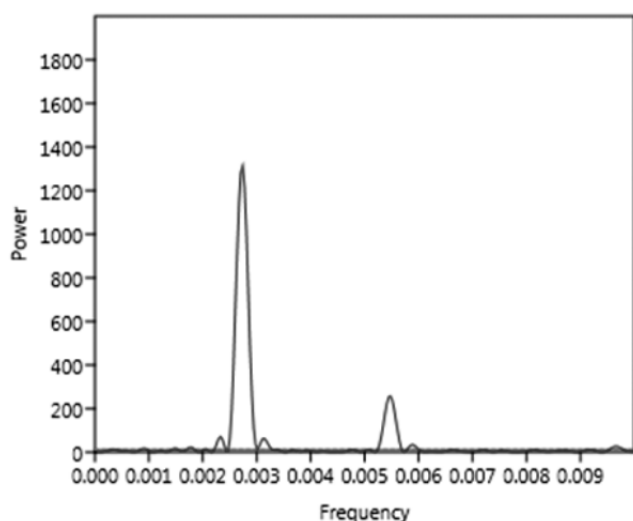


**Fig. 8.** Periodogram of long-term series of surface ozone concentrations.

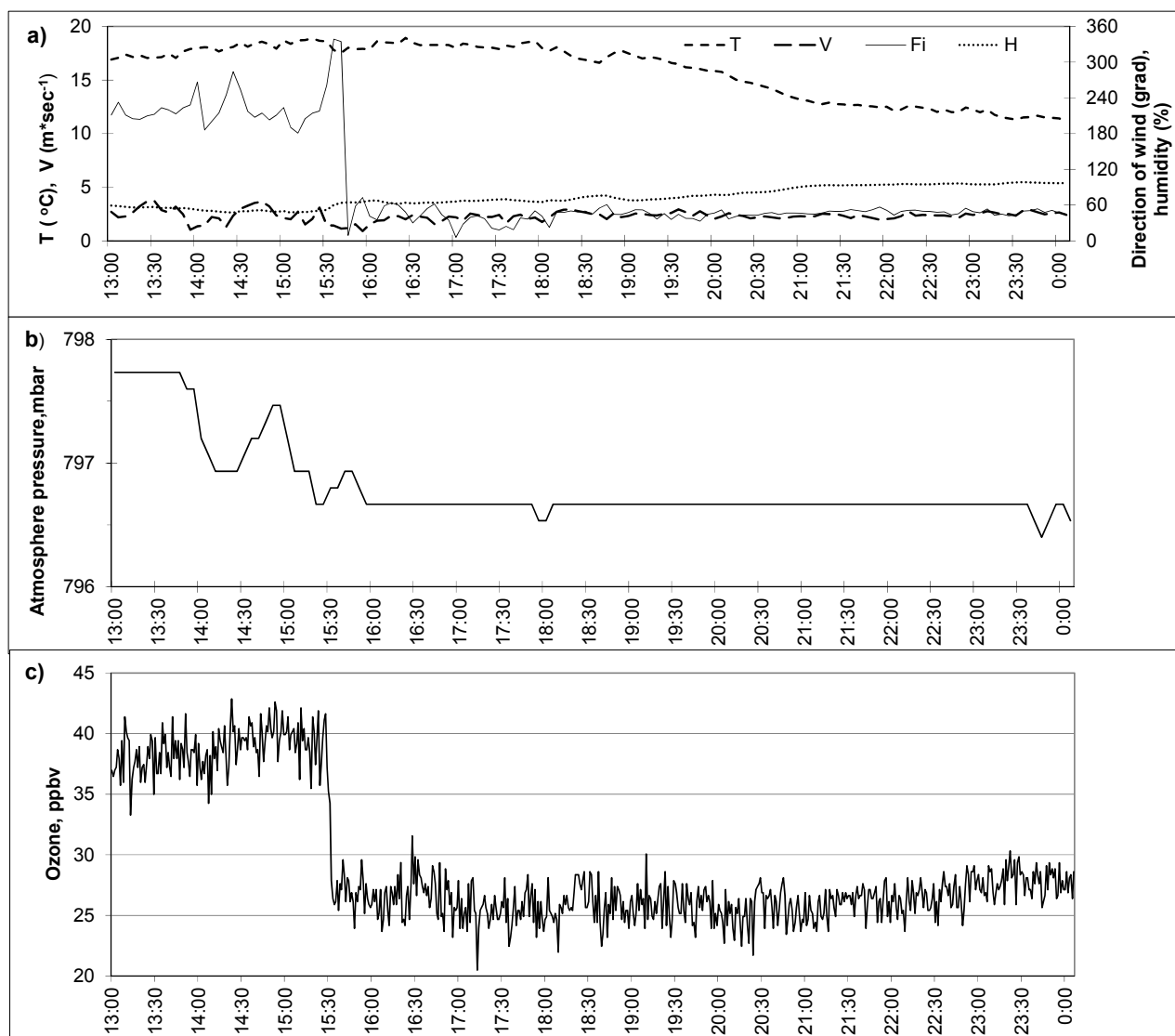


**Fig. 9.** Effect of wind direction Fi ((a), right axis) on (c) ozone concentration; July 9, 2007, local time (T: air temperature; V: wind speed; Fi: wind direction; H: air humidity).

Central Asia (Lee *et al.*, 2011; Loshchenko and Latysheva, 2015). Dust dominates in the total atmospheric load of the Asian countries: approximately 70% for China and Mongolia, 60% for Korea, 50% for Japan and 40% for the Northern Pacific Ocean (Tanaka, Chiba, 2006). With the distance from the source, dust particles are enriched with pollutants from the atmosphere and, as a result, chemical composition of the original aerosol particles changes (Geng *et al.*, 2014). Hence, any impact of either anthropogenic or natural character on air changes chemical composition of aerosol particularly in the background area. Semi-desert and desert regions of Mongolia and China with brown humus soils with significant distribution of saline lands and sands are the sources for  $\text{Cl}^-$ ,  $\text{K}^+$  and  $\text{Na}^+$  (Lopatovskaya and Sugachenko, 2010). For example, in the northwestern region of China at the site Aksu (saline lands with brown soil), aerosol contained calcite ( $\text{CaCO}_3$ ), halite ( $\text{NaCl}$ ) and gypsum ( $\text{CaSO}_4 \cdot 2\text{H}_2\text{O}$ ). The dissolved fraction of this aerosol was dominated by  $\text{SO}_4^{2-}$ ,  $\text{NO}_3^-$ ,  $\text{Cl}^-$ ,  $\text{NH}_4^+$ ,  $\text{Ca}^{2+}$ , and  $\text{Na}^+$  (Yabuki *et al.*, 2005).

In the seasonal dynamics of  $\text{SO}_4^{2-}$ , there are three maxima, which coincided with synoptic processes. The first rise of this ion was recorded in February–March during the destruction of the Asian anticyclone and, as a result, the concentrations of terrigenous material increased in the surface atmosphere with the intensification of wind and thawing of the snow cover. The second maximum was registered in late May–July, when turbulent heat exchange convection in the atmosphere intensified at intense solar radiation. The third  $\text{SO}_4^{2-}$  maximum was observed in autumn (October–November), when cyclogenesis became more active again during transformation of the pressure field from the summer to winter type near the earth. Main maxima are in good agreement with the annual trend of wind speed coinciding in time with relatively dry periods. Maximal concentrations of  $\text{Cl}^-$  and  $\text{Na}^+$  were recorded in late July–August because of the frequent deep cyclones from Mongolia staying for a long time in the south of Pribaikalye.

**Table 3.** Seasonal average long-term concentrations, mean square deviations of concentrations of major ions in aerosol at site Mondy during 2000–2017,  $\mu\text{g m}^{-3}$ .

	$\text{SO}_4^{2-}$	$\text{NO}_3^-$	$\text{Cl}^-$	$\text{NH}_4^+$	$\text{Na}^+$	$\text{K}^+$	$\text{Mg}^{2+}$	$\text{Ca}^{2+}$	Sum of ions
January	$0.42 \pm 0.32$	$0.03 \pm 0.04$	$0.06 \pm 0.13$	$0.12 \pm 0.11$	$0.03 \pm 0.03$	$0.02 \pm 0.02$	$0.01 \pm 0.01$	$0.06 \pm 0.05$	$0.75 \pm 0.71$
February	$0.60 \pm 0.51$	$0.04 \pm 0.04$	$0.05 \pm 0.10$	$0.14 \pm 0.15$	$0.04 \pm 0.05$	$0.05 \pm 0.06$	$0.01 \pm 0.01$	$0.07 \pm 0.06$	$1.00 \pm 0.97$
March	$0.49 \pm 0.42$	$0.04 \pm 0.06$	$0.09 \pm 0.18$	$0.15 \pm 0.15$	$0.06 \pm 0.14$	$0.04 \pm 0.06$	$0.01 \pm 0.01$	$0.06 \pm 0.05$	$0.94 \pm 1.06$
April	$0.47 \pm 0.49$	$0.02 \pm 0.03$	$0.05 \pm 0.08$	$0.14 \pm 0.20$	$0.06 \pm 0.12$	$0.04 \pm 0.06$	$0.01 \pm 0.01$	$0.05 \pm 0.05$	$0.84 \pm 1.03$
May	$0.50 \pm 0.38$	$0.05 \pm 0.05$	$0.04 \pm 0.07$	$0.14 \pm 0.13$	$0.03 \pm 0.03$	$0.05 \pm 0.07$	$0.01 \pm 0.01$	$0.06 \pm 0.06$	$0.88 \pm 0.81$
June	$0.68 \pm 0.88$	$0.09 \pm 0.13$	$0.04 \pm 0.05$	$0.16 \pm 0.26$	$0.04 \pm 0.05$	$0.08 \pm 0.10$	$0.01 \pm 0.01$	$0.08 \pm 0.06$	$1.18 \pm 1.53$
July	$0.43 \pm 0.39$	$0.05 \pm 0.08$	$0.09 \pm 0.18$	$0.10 \pm 0.15$	$0.07 \pm 0.10$	$0.07 \pm 0.09$	$0.01 \pm 0.02$	$0.06 \pm 0.05$	$0.88 \pm 1.06$
August	$0.31 \pm 0.23$	$0.12 \pm 0.26$	$0.15 \pm 0.41$	$0.06 \pm 0.06$	$0.11 \pm 0.25$	$0.05 \pm 0.05$	$0.01 \pm 0.02$	$0.06 \pm 0.05$	$0.87 \pm 1.34$
September	$0.30 \pm 0.21$	$0.11 \pm 0.27$	$0.02 \pm 0.03$	$0.07 \pm 0.07$	$0.02 \pm 0.02$	$0.04 \pm 0.04$	$0.00 \pm 0.00$	$0.04 \pm 0.03$	$0.60 \pm 0.67$
October	$0.29 \pm 0.20$	$0.02 \pm 0.02$	$0.03 \pm 0.04$	$0.06 \pm 0.05$	$0.02 \pm 0.02$	$0.04 \pm 0.05$	$0.01 \pm 0.01$	$0.04 \pm 0.04$	$0.51 \pm 0.42$
November	$0.32 \pm 0.19$	$0.03 \pm 0.04$	$0.02 \pm 0.03$	$0.08 \pm 0.08$	$0.02 \pm 0.02$	$0.02 \pm 0.01$	$0.00 \pm 0.00$	$0.04 \pm 0.03$	$0.53 \pm 0.40$
December	$0.28 \pm 0.18$	$0.06 \pm 0.08$	$0.10 \pm 0.20$	$0.09 \pm 0.09$	$0.04 \pm 0.08$	$0.03 \pm 0.04$	$0.00 \pm 0.00$	$0.04 \pm 0.03$	$0.64 \pm 0.70$

Inter-annual variability of gaseous impurities ( $\text{SO}_2$ ,  $\text{HNO}_3$  and  $\text{NH}_3$ ) in the atmosphere at site Mondy was estimated from the data of measurements obtained in 2000–2017. Sulfur dioxide ( $\text{SO}_2$ ) and ammonia ( $\text{NH}_3$ ) were dominant gases in atmosphere. Inter-annual trend of concentrations of impurities and average inter-annual negative temperature was calculated as arithmetic mean of average monthly air temperature in January, February, March, October, November, and December, when air temperature was negative (Table 5). Inter-annual dynamics of gases depended on dynamics of negative temperatures. For example, concentrations of  $\text{SO}_2$  and  $\text{HNO}_3$  increased at lower temperatures, whereas the concentrations of  $\text{NH}_3$  decreased, although the degree of variability of their concentrations was disproportional to variability of changes of average temperature.

Three maxima were recorded in the annual trend of  $\text{SO}_2$  as well as of  $\text{SO}_4^{2-}$ : in winter (February), summer (July) and in autumn–winter period (November–December). Low ratio of  $\text{SO}_4^{2-}/\text{SO}_2$  ( $0.18 \div 0.75$ ) concentrations at site Mondy attested to the absence of anthropogenic sources of sulfate in the atmosphere.

The annual trend of  $\text{HNO}_3$  concentration from January to August was close to the dynamics of  $\text{SO}_2$ . However, the third maximum of  $\text{HNO}_3$  concentrations unlike that of  $\text{SO}_2$  was registered in September. In the autumn–winter period, the concentrations of  $\text{HNO}_3$  reduced. The ratio of  $\text{NO}_3^-/\text{HNO}_3$  concentrations was higher ( $0.18 \div 1.17$ ) than that of sulfur compounds (in August and December, the ratio was higher than 1). The annual trend of  $\text{NH}_3$  concentrations was typical of other continental regions with its maximum in the warm period. The ratio of  $\text{NH}_4^+/\text{NH}_3$  concentrations was the lowest in August and the highest in February varying within the  $0.07 \div 0.45$  range. Such a ratio attests that the emission of  $\text{NH}_3$  of natural origin is higher than the rate of its transformation into aerosol.

## CONCLUSIONS

We analyzed the dynamics of the ozone, gaseous impurities and ionic composition of the aerosol for a long period of observations (2000–2017) performed at the alpine site Mondy, which is part of the international EANET program. Based on the long-term results, this site may be regarded as a representative background site for the vast region of Central Asia.

The maximal concentrations of ozone were recorded in April and early May, whereas the minimal concentrations were recorded in July and August. The diurnal SOC dynamics exhibited the following characteristics:

- The minimal diurnal variability, with an amplitude of 0.9 ppb, was recorded in January.
- The maximal diurnal variability, with an amplitude of 5 ppb, was recorded in July.
- Diurnal variations in April and October were similar, with amplitudes of 2 ppb.

We examined abrupt changes in meteorological conditions in the alpine region, which affected the composition of the surface-level ozone. A sharp increase or decrease in the

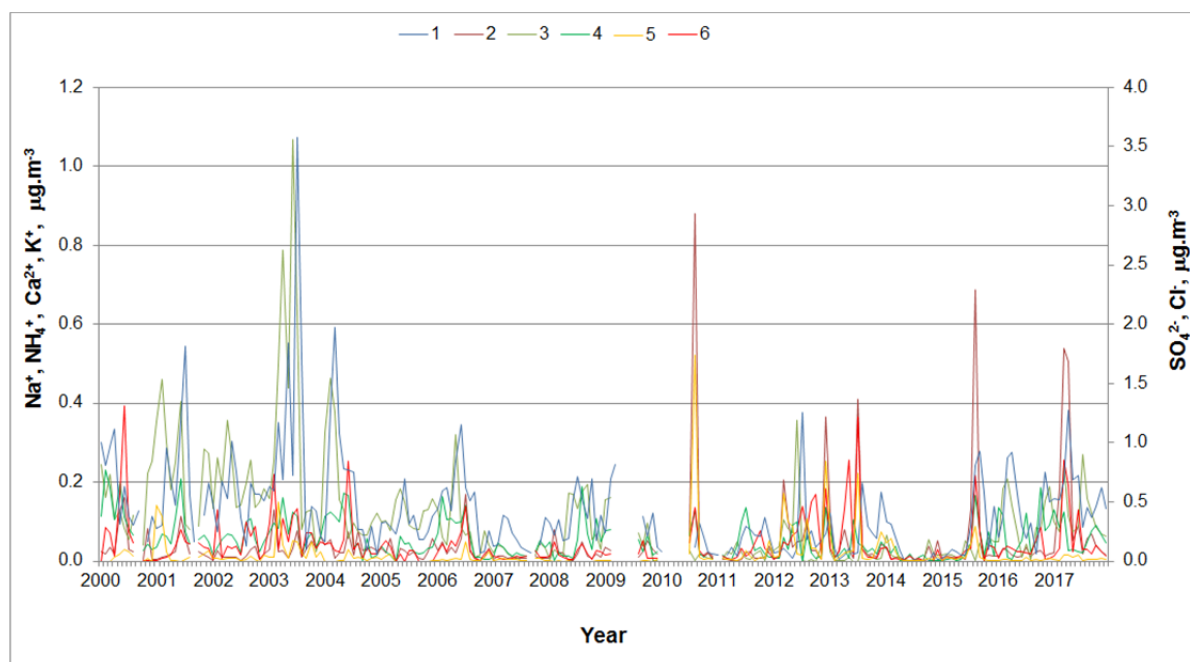


**Fig. 10.** Inter-annual variability of ion concentrations ( $\mu\text{g m}^{-3}$ ) in aerosol in 2000–2017. 1:  $\text{SO}_4^{2-}$ , 2:  $\text{Na}^+$ , 3:  $\text{NH}_4^+$ , 4:  $\text{Ca}^{2+}$ , 5:  $\text{Cl}^-$ , 6:  $\text{K}^+$ .

**Table 4.** Variation ranges of average long-term concentrations (min–max), average long-term concentrations ( $\bar{x}$ ), mean square deviations of concentrations ( $\sigma$ ) of major ions in aerosol at site Mondy during different periods of measurements,  $\mu\text{g m}^{-3}$ .

Ion/Period	2000–2009		2010–2015	
	min ÷ max	$\bar{x} \pm \sigma$	min ÷ max	$\bar{x} \pm \sigma$
$\text{NH}_4^+$	0.021 ÷ 0.355	$0.151 \pm 0.098$	0.010 ÷ 0.067	$0.026 \pm 0.023$
$\text{Ca}^{2+}$	0.026 ÷ 0.109	$0.063 \pm 0.025$	0.012 ÷ 0.046	$0.036 \pm 0.012$
$\text{SO}_4^{2-}$	0.219 ÷ 0.972	$0.522 \pm 0.215$	0.062 ÷ 0.309	$0.195 \pm 0.088$
$\text{Na}^+$	0.009 ÷ 0.048	$0.029 \pm 0.012$	0.011 ÷ 0.169	$0.071 \pm 0.057$
$\text{K}^+$	0.011 ÷ 0.083	$0.040 \pm 0.025$	0.010 ÷ 0.082	$0.046 \pm 0.029$
$\text{Cl}^-$	0.002 ÷ 0.120	$0.036 \pm 0.042$	0.042 ÷ 0.312	$0.138 \pm 0.114$

**Table 5.** Inter-annual concentrations of gaseous impurities ( $\mu\text{g m}^{-3}$ ) and average air temperatures in winter period (January–March, October–December).

	$\text{HNO}_3$	$\text{HCl}$	$\text{NH}_3$	$\text{SO}_2$	$T, ^\circ\text{C}$
2000	0.12	0.07	0.47	0.20	–16.1
2001	0.46	0.63	0.33	0.46	–19.6
2002	0.10	0.06	0.53	0.28	–18.5
2003	0.17	0.24	0.57	0.55	–13.8
2004	0.10	0.25	0.30	0.54	–14.9
2005	0.19	0.08	0.54	3.16	–19.3
2006	0.02	0.11	1.34	1.76	–16.9
2007	0.08	0.05	0.71	0.92	–16.0
2008	0.09	0.07	0.48	0.75	–15.8
2009	0.00	0.00	0.29	0.41	–20.7
2010	0.59	0.79	0.26	1.43	–19.6
2011	0.05	0.60	0.26	0.33	–18.4
2012	0.27	1.02	0.48	1.59	–21.5
2013	0.09	1.12	0.45	0.33	–18.4
2014	0.04	1.39	0.26	0.34	–17.8
2015	0.04	1.39	0.26	0.34	–15.5
2016	0.07	2.37	1.03	0.29	–17.2
2017	0.10	3.96	0.71	0.50	–14.6

SOC occurred when the wind direction changed (for several minutes), which has not been observed in other regions with flat landscapes. No positive trend was displayed by the SOC at this monitoring site during the entire period of observation.

From 2000 to 2009, the major ions in the aerosol at Mondy were  $\text{NH}_4^+$ ,  $\text{Ca}^{2+}$  and  $\text{SO}_4^{2-}$ . From 2010 to 2015, the  $\text{NH}_4^+$  and  $\text{SO}_4^{2-}$  decreased while the  $\text{Cl}^-$ ,  $\text{Na}^+$  and  $\text{K}^+$  increased. In our opinion, the main reason for this change is the intensified aridization of climate and rise of dust storms in Central Asia. Similar seasonal dynamics for the gaseous impurities of sulfur and nitrogen and for the major ions were recorded for the aerosol. Among the gaseous impurities, the highest concentrations were registered for  $\text{NH}_3$  and  $\text{SO}_2$ .

## ACKNOWLEDGEMENTS

This study was supported by State Project 00345-2016-0008 (expeditionary work and data interpretation) and Russian Foundation for Basic Research (RFBR) project 17-29-05044 (chemical data analysis).

## REFERENCES

- Akimoto, N. (2006). *Tropospheric ozone a growing threat*. Acid Deposition and Oxidant Research Center, Niigata, Japan. 26 p.
- Aldaz, L. (1969). Flux measurement of atmospheric ozone over land and water. *J. Geophys. Res.* 74: 6943–6946.
- Bashurova, V.S., Dreiling, V., Hodger, T.V., Jaenicke, R., Koutsenogii, K.P., Koutsenogii, P.K., Kraemer, M., Makarov, V.I., Obolkin, V.A., Potjomkin, V.L. and Pusep, A.Y. (1992). Measurements of atmospheric condensation nuclei size distributions in Siberia. *J. Aerosol Sci.* 23: 191–199.
- Belan, B.D. (2010). *Ozone in troposphere*. Tomsk: Institute of Atmosphere Optics. SB RAS, 487 p. (in Russian).
- Chen, B.B., Imashev, S.A., Sverdlik, L.G., Solomon, P.A., Lantz, J., Schauer, J.J., Shafer, M.M., Artamonova, M.S. and Carmichael, G.R. (2013). Ozone variations over central Tien-Shan in Central Asia and implications for regional emissions reduction strategies. *Aerosol Air Qual. Res.* 13: 555–562.
- EANET (1998-2015). Report of the inter-laboratory comparison project, <http://www.eanet.asia/product/index.html>, Last Access: 17 March 2018.
- Geng, H., Hwang, H., Liu, X., Dong, S. and Ro, C.U. (2014). Investigation of aged aerosols in size-resolved Asian dust storm particles transported from Beijing, China, to Incheon, Korea, using low-Z particle EPMA. *Atmos. Chem. Phys.* 14: 3307–3323.
- Gilge, S., Plass-Duelmer, C., Fricke, W., Kaiser, A., Ries, L., Buchmann, B. and Steinbacher, M. (2010). Ozone, carbon monoxide and nitrogen oxides time series at four alpine GAW mountain stations in central Europe. *Atmos. Chem. Phys.* 10: 12295–12316.
- Habeebullah, T.M.A. (2016). Chemical Composition of particulate matters in Makkah – Focusing on cations, anions and heavy metals. *Aerosol Air Qual. Res.* 16: 336–347.
- Izrael, Y.A., Nazarov, I.M., Pressman, A.Y., Filippova, L.M. and Ryaboshapko, A. G. (1989). *Acid rains*. Gidrometeoizdat, Leningrad, Russia. (in Russian).
- Karlsson, P.E., Tang, L., Sundberg, J., Chen, D., Lindskog, A. and Pleijel, H. (2007). Increasing risk for negative ozone impacts on vegetation in northern Sweden. *Environ. Pollut.* 150: 96–106.
- Laurila, T. (1999). Observational study of transport and photochemical formation of ozone over northern Europe. *J. Geophys. Res.* 104: 26235–26243.
- Lee, E.H. and Sohn, B.J. (2011). Recent increasing trend in dust frequency over Mongolia and Inner Mongolia regions and its association with climate and surface condition change. *Atmos. Environ.* 45: 4611–4616.
- Lopatovskaya, O.G. and Sugachenko, A.A. (2010). *Soil melioration. Saline soils*. Irkutsk State University, Irkutsk, Russia, p. 101 (in Russian).
- Loshchenko, K.A. and Latysheva, I.V. (2015). Regional characteristics of synoptic processes in the territory of Irkutsk Region in 2000–2013. *Bull. Irkutsk State Univ.* 11: 38–54 (in Russian).
- Monks P. (2000). A review of the observations and origins of the spring ozone maximum. *Atmos. Environ.* 34: 3545–3561.
- Obolkin, V.A., Khodzher, T.V., Anokhin, Y.A. and Prokhorova, T.A. (1991). Acidity of atmospheric precipitation in the Lake Baikal region. *Meteorol. Hydrol.* 1: 55–60 (in Russian).
- Osada, K., Kido, M., Nishita, C., Matsunaga, K., Iwasaka, Y., Nagatani, M. and Nakada, H. (2002). Changes in ionic constituents of free tropospheric aerosol particles obtained at Mt. Norikura (2770 m a.s.l.), central Japan, during the Shurin period in 2000. *Atmos. Environ.* 36: 5469–5477.
- Ozville, R. (1967). Ozone production during thunderstorms measured by the absorption of ultraviolet radiation from lightning. *J. Geophys. Res.* 77: 3557–3561.
- Pochanart P., Akimoto H., Khodzher T., Kajii Y. and Potemkin V. (2003). Regional background ozone and carbon monoxide variations in remote Siberia (East Asia). *J. Geophys. Res.* 108: 4028.
- Preunkert S., Wagenbach D. and Legran M. (2002). Improvement and characterization of an automatic aerosol sampler for remote (glacier) sites. *Atmos. Environ.* 36: 1221–1232.
- Reddy, B.S.K., Kumar, K.R., Balakrishnaiah, G., Gopal, K.R., Reddy, R.R., Sivakumar, V., Lingaswamy, A.P., Arafath, S.Md., Umadevi, K., Kumari, S.P., Ahammed, Y.N. and Lal, S. (2012). Analysis of diurnal and seasonal behavior of surface ozone and its precursors ( $\text{NO}_x$ ) at a semi-arid rural site in Southern India. *Aerosol Air Qual. Res.* 12: 1081–1094.
- Ren, L., Zhang, R., Bai, Z., Chen, J., Liu, H., Zhang, M., Yang, X. and Zhang L. (2012). Aircraft measurements of ionic and elemental components in  $\text{PM}_{2.5}$  over eastern coastal area of China. *Aerosol Air Qual. Res.* 12: 1237–1246.

- Rovinsky, F.Y. and Egorov, V.I. (1986). *Ozone, oxides of nitrogen and sulphur in the lower atmosphere*. L.: Hydrometeoizdat. 183 p. 101 (in Russian).
- Sandroni, S., Baci, P., Boffa, G., Pellegrini, U. and Ventura, A. (1994) Tropospheric ozone in the pre-alpine and alpine regions. *Sci. Total Environ.* 156: 169–182.
- Tanaka, T.Y. and Chiba, M. (2006). A numerical study of the contributions of dust source regions to the global dust budget. *Global Planet. Change* 52: 88–104.
- Technical Manual on Dry Deposition Flux Estimation in East Asia (2003). <http://www.eanet.asia/product/index.html>, Last Access: 17 January 2017.
- Turner, N.C., Rich, S. and Waggoner, P.E. (1980). Removal of ozone by soil. *Environ. Qual.* 2: 259–264.
- Wesely, M.L., Cook, D.R. and Williams, R.M. (1981). Fields measurement of small ozone fluxes to snow, wet bare soil and the water. *Boundary Layer Meteorol.* 20: 459–264.
- Yabuki, S., Mikami, M., Nakamura, Y., Kanayama, S., Fu, F., Liu, M. and Zhou, H. (2005). The characteristics of atmospheric aerosol at Aksu, an Asian dust-source region of north-west China: A summary of observations over the three years from March 2001 to April 2004. *J. Meteor. Soc. Japan* 83A: 45–72.
- Zanis, P., Ganser, A., Zellweger, C., Henne, S., Steinbacher, M. and Staehelin, J. (2007). Seasonal variability of measured ozone production efficiencies in the lower free troposphere of Central Europe. *Atmos. Chem. Phys.* 7: 223–236.

*Received for review, June 4, 2018*

*Revised, September 3, 2018*

*Accepted, October 30, 2018*